

# Mitochondrial Fragmentation Leads to Intracellular Acidification in *Caenorhabditis elegans* and Mammalian Cells

David Johnson\* and Keith Nehrke<sup>†‡</sup>

Departments of \*Biochemistry, <sup>†</sup>Medicine, and <sup>‡</sup>Pharmacology and Physiology, University of Rochester Medical Center, Rochester, NY 14642

Submitted October 19, 2009; Revised April 20, 2010; Accepted April 22, 2010  
Monitoring Editor: M. Bishr Omary

Mitochondrial structural dynamics are regulated through the opposing processes of membrane fission and fusion, which are conserved from yeast to man. The chronic inhibition of mitochondrial fusion as a result of genetic mutation is the cause of human autosomal dominant optic atrophy (ADOA) and Charcot-Marie-Tooth syndrome type 2A (CMT-2A). Here, we demonstrate that genetic fragmentation of the mitochondrial network in *Caenorhabditis elegans* induces cellular acidification in a broad range of tissues from the intestine, to body wall muscles, and neurons. Genetic epistasis analyses demonstrate that fragmentation itself, and not the loss of a particular protein, leads to acidosis, and the worm's fitness matches the extent of acidification. We suggest that fragmentation may cause acidification through two distinct processes: oxidative signaling after the loss of the ability of the mitochondrial inner membrane to undergo fusion and lactic acidosis after the loss of outer membrane fusion. Finally, experiments in cultured mammalian cells demonstrate a conserved link between mitochondrial morphology and cell pH homeostasis. Taken together these data reveal a potential role for acidosis in the differing etiology of diseases associated with mitochondrial morphology defects such as ADOA and CMT-2A.

## INTRODUCTION

Mitochondria have long been known as the primary site of energy production in aerobic eukaryotic cells. The observation that mitochondria undergo drastic structural changes during development was reported as early as 1931 (Smith, 1931). However the molecular basis of these changes was incompletely understood until the discovery of a conserved mitochondrial GTPase FZO1 that is necessary for mitochondrial fusion in the Nebenkern structure of *Drosophila* sperm (Hales and Fuller, 1997). Subsequently, the processes of mitochondrial fission and fusion were found to be controlled by a number of proteins that are conserved from yeast to mammals. The mitochondrial matrix is separated from the cell's cytoplasm by two membranes, and both the inner and outer membranes are structurally regulated during morphological changes. Thus, the proteins that regulate mitochondrial dynamics include the outer membrane GTPases MFN1 and MFN2 (Hales and Fuller, 1997; Hermann *et al.*, 1998; Santel and Fuller, 2001), the inner membrane GTPase OPA1 (Shepard and Yaffe, 1999; Alexander *et al.*, 2000; Delettre *et al.*, 2000), the cytosolic factor DRP1 (Otsuga *et al.*, 1998; Smirnova *et al.*, 1998), and its outer membrane-bound adapter FIS1 (Mozdy *et al.*, 2000; James *et al.*, 2003; Yoon *et al.*, 2003). Fission and fusion are tightly regulated, particularly during mitochondrial transport and turnover, and may contribute to the maintenance and function of the organelle, as well (Li *et al.*, 2004; Chen *et al.*, 2005, 2007; Kowald *et al.*,

2005; Benard *et al.*, 2007; Misgeld *et al.*, 2007; Twig *et al.*, 2008). Recently, it has been suggested that mitochondrial fragmentation is an important aspect of the apoptotic cell death cascade in mammals (Breckenridge *et al.*, 2003; Lee *et al.*, 2004), though whether this is evolutionarily conserved is unclear.

Not surprisingly, the inability to control mitochondrial morphology has been shown to cause disease in humans. Mutations in the human profusion gene *OPA1* (Olichon *et al.*, 2002) cause autosomal-dominant optic atrophy (ADOA), a disease characterized by progressive blindness due to the loss of retinal ganglion cells and optic nerve atrophy (Delettre *et al.*, 2000). Mutations in *MFN2*, which encodes one of two *mitofusin* proteins (Santel and Fuller, 2001), lead to the peripheral neuropathy Charcot-Marie-Tooth syndrome type 2A (CMT-2A; Zuchner *et al.*, 2004). Although it has been clearly demonstrated that mutations in these genes are causally linked to disease, their pathogenic mechanism remains unclear. These diseases commonly result from haplo-insufficiency, where a single functional copy of the gene does not produce enough protein to bring about a wild-type condition, or a dominant negative mutation, where a mutated version of the protein interferes with the wild-type copy. Regardless, it is not currently understood how the loss of *OPA1* or *MFN2* activity in these diseases are causally linked to cell dysfunction and/or death or why the damage is restricted to particular neuronal tissues despite the ubiquitous expression of both proteins.

Because the primary function of mitochondria in most eukaryotic cells is the production of energy through oxidative phosphorylation, it has been suggested that the excessive fragmentation of the mitochondria caused by these mutations reduces energy production and likely affects neurons because of their high energy demands. Indeed it has been confirmed in cell culture that inducing mitochondrial

This article was published online ahead of print in *MBoC in Press* (<http://www.molbiolcell.org/cgi/doi/10.1091/mbc.E09-10-0874>) on May 5, 2010.

Address correspondence to: Keith Nehrke ([keith\\_nehrke@urmc.rochester.edu](mailto:keith_nehrke@urmc.rochester.edu)).

fragmentation can lead to the loss of membrane potential, slowed growth, and defective oxidative phosphorylation (Chen *et al.*, 2005; Zanna *et al.*, 2008). However, despite the defects in mitochondrial energy production, AMP/ATP ratios under fragmented conditions remain constant, possibly indicating a switch to alternative means of energy production to maintain energy homeostasis (Baloh *et al.*, 2007; Zanna *et al.*, 2008). Furthermore, recent evidence suggests that a loss of energy (i.e., ATP) is not the primary cause of disease, as a novel mutation in the GTPase domain of OPA1 has been isolated from a family of ADOA sufferers that alters mitochondrial distribution, yet has no effect on mitochondrial ATP production (Spinazzi *et al.*, 2008). Other hypotheses for how fragmentation leads to disease incorporate concepts such as improper mitochondrial localization due to poor trafficking in the absence of the ability to regulate morphology or reduced mitochondrial Ca<sup>2+</sup> buffering (Spinazzi *et al.*, 2008). However, definitive evidence supporting these hypotheses is lacking.

The lethal nature of homozygous deletions of *MFN2* and *OPA1* genes in mice has confounded research and made it necessary to study many aspects of mitochondrial dynamics in cell culture or using heterozygous mutant and conditional knockout populations (Chen *et al.*, 2005; Davies *et al.*, 2007). In contrast, the core protein machinery involved in mitochondrial remodeling is remarkably similar in the nematode *Caenorhabditis elegans* to that in mammals with the exception that homozygous deletions of the genes involved in the regulation of these processes are tolerated (Kanazawa *et al.*, 2008; Tan *et al.*, 2008).

In this article we utilize the unique advantages of the nematode model system to demonstrate that fragmentation of the mitochondrial network is sufficient to induce robust cellular acidification. Using a combination of genetics, integrative physiology, and conventional biochemistry, we examine the tissue specificity of this phenotype and its dependence on the nature of the molecular lesion. Finally, we demonstrate that fragmentation of the mitochondrial network in cultured mammalian cells by either depletion of OPA1 through the application of short-interfering RNAs (siRNAs) or by overexpression of a dominant hFis1 also causes intracellular acidification, suggesting conservation between phyla. Our results lead to the hypothesis that cellular acidification may play a role in both the tissue specificity and progression of fusion-related diseases such as ADOA and CMT-2A.

## MATERIALS AND METHODS

**Strains, Vectors, and Culturing Techniques.** *C. elegans* were cultured using standard techniques at 20°C on normal growth media-agar plates (Brenner, 1974). For imaging studies the worms were transferred to plates with agarose substituted for agar to reduce background fluorescence. The wild-type strain is Bristol N2. The *eat-3(tm1107)*, *fzo-1(tm1133)*, and *drp-1(tm1108)* alleles were generated by Dr. Shohei Mitani with the Japanese Bioresource Project. The *eat-3(ad426)* strain was created by Dr. Leon Avery. The *eat-3(ad426)*; *drp-1(cq5)* mutant and all strains (except N2) were generously provided by Dr. Alex van der Bliek (University of California at Los Angeles). All mutant alleles were extensively outcrossed before their use.

The intestinal-specific pH sensor used in this work has been described (Nehrke, 2003; Pfeiffer *et al.*, 2008). The other tissue-specific pH sensor constructs were generated by fusing the upstream promoter regions of *myo-3* and *calh-4a* to the pH-sensitive GFP variant pHluorin to measure muscular and neuronal pH, respectively. Promoter regions used were the ~2-kb upstream region of *myo-3* and ~400 nucleotides upstream of the *calh-4* translational start site for *calh-4a*. The *myo-3* promoter region was amplified from genomic DNA using primers (IDT, Coralville, IA) tagged with NheI and SacII restriction sites on the forward and reverse primers, respectively, and was then cloned into the NheI-SacII sites of the pHluorin encoding vector pIA3 to generate pDJ4 (*Pmyo-3::pHluorin*). The *calh-4a* promoter was fused to pHluorin via PCR to generate (*Pcalh-4::pHluorin*). The mitochondria targeted redox sensor was

generated through site-directed mutagenesis of the wild-type green fluorescent protein (GFP) chromophore, as described (Hanson *et al.*, 2004). This GFP variant (roGFP1) contains the mutations C48S, F64L, S65T, Q80R, S147C, Q204C, and F223K. It was expressed in the pFH6.II vector and tagged with a 150-nucleotide aspartyl transferase mitochondrial targeting signal (MTS). The location of the reporter to the mitochondria was confirmed by confocal micrography; in addition, fusion of the MTS to the pH sensor protein pHluorin resulted in pH measurements of >7.8, suggesting mitochondrial targeting (data not shown). The *myo-3* promoter discussed above was used to drive muscle-specific expression and was cloned into the NheI-SacII sites of pFH6.II (pDJ7). Rescue of *eat-3* loss-of-function (lf) was accomplished by expression of a genomic fragment encompassing the promoter region, open-reading frame, and 3' untranslated region (UTR) of the *eat-3* gene (*Peat-3::EAT-3* PCR). The hFis1 overexpression construct was a kind gift from Dr. Y. Yoon (University of Rochester) and has been described previously (Serasinghe and Yoon, 2008). The catalase overexpressing strain was a kind gift from Dr. David Gems (University College London) and has been described, as well (Doonan *et al.*, 2008).

Constructs were microinjected into the gonad of young adult *pha-1(e2123ts)*; *him-5(e1490)* along with pCL1, which rescues the temperature-sensitive pharyngeal development defect of the *pha-1(e2123ts)* allele. Transgenic lines were established and used as the wild-type controls for subsequent experiments. Transgenic males from established lines were mated against mutant hermaphrodites to generate transgenic mutant lines. The mutations themselves were followed using either visible phenotypes or genomic PCR with primers flanking the deleted regions.

The strains areas were as follows: KWN36: *pha-1(e2123ts)III* myEx006[pIA5*nhrx-2(Pnhrx-2::pHluorin)*]; pCL1(*pha-1+*), KWN47: *eat-3(ad426)II*, *pha-1(e2123ts)III* myEx006; KWN62: *eat-3(tm1107)II*, *pha-1(e2123ts)III* myEx006; KWN125: *fzo-1(tm1133)II*, *pha-1(2123ts)III*, *him-5(e1490)V* myEx006 KWN159: *drp-1(tm1108)IV*, *pha-1(e2123ts)III*, *him-5(e1490)V* myEx006; KWN67: *pha-1(e2123ts)III*, *him-5(e1490)V* myEx034[pDJ4(*Pmyo-3::pHluorin*)]; pCL1; KWN137: *fzo-1(tm1133)II*, *pha-1(e2123ts)III*, *him-5(e1490)V* myEx034; KWN154: *eat-3(ad426)II*, *pha-1(e2123ts)III*, *him-5(e1490)V* myEx034; KWN155: *eat-3(tm1107)II*, *pha-1(e2123ts)III*, *him-5(e1490)V* myEx034; KWN158: *eat-3(ad426)II*, *drp-1(cq5)IV* myEx080[pDJ4, pCL1]; KWN119: *pha-1(e2123ts)III*, *him-5(e1490)V* myEx061[pDJ7(*Pmyo-3::mito-redoxGFP*)]; pCL1; KWN134: *fzo-1(tm1133)II*, *pha-1(e2123ts)III*, *him-5(e1490)V* myEx061; KWN156: *eat-3(ad426)II*, *pha-1(e2123ts)III*, *him-5(e1490)V* myEx061; KWN157: *eat-3(tm1107)II*, *pha-1(e2123ts)III*, *him-5(e1490)V* myEx079[*Peat-3::EAT-3* PCR]; pDJ4; pCL1; KWN172: *pha-1(2123ts)III*, *him-5(e1490)V* myEx096[*Pcalh-4a::pHluorin* PCR]; pCL1; KWN173: *eat-3(tm1107)II*, *pha-1(2123ts)III*, *him-5(e1490)V* myEx096; KWN174: *fzo-1(tm1133)II*, *pha-1(2123ts)III*, *him-5(e1490)V* myEx096.

**RNA Interference, Redox, and pH Imaging In Vivo.** Fresh transformations of each RNA interference (RNAi) vector, including the control vector pPD129.36, which does not have an insert, were grown in the *Escherichia coli* HT115 strain to midlog phase at 37°C and then induced for 1 h with 1 mM IPTG. After fivefold concentration 100 μl of bacteria was added to the surface of 35-mm NGM agar plates supplemented with cholesterol and IPTG. For dichloroacetate supplementation 5 mg/ml sodium dichloroacetate were added to the plates. Two days later L3 larvae were placed onto the RNAi plates and were allowed to mature to adulthood and lay eggs for 12–24 h. The pH of the indicated cells within the transgenic progeny was assessed as follows: L3 progeny were transferred to a 60-mm NGM agarose plate lightly seeded with OP50 (to reduce background). After a 1–2-h equilibration period worms were imaged via a high NA, 20× Nikon Plan Apo (Nikon, Melville, NY) objective, with fluorescent emissions monitored at 535 nm after high-speed dual excitation at 410 and 470 nm. Mitochondrial redox imaging was accomplished using an identical technique with the exception that worms were imaged under a coverslip on a 2% M9 agarose pad in M9 containing 0.1% tetramisole (Sigma-Aldrich, St. Louis, MO) and 0.1% tricaine (EMS, Hatfield, PA). Illumination was provided by a Polychrome V monochromator (TILL Photonics, Martinsreid, Germany) rigged to a Nikon Eclipse TE2000-S inverted microscope equipped with a high-speed CCD camera (Cooke, Kelheim, Germany). Regions of interest (ROIs) were outlined using INDEC Imaging Workbench 5.1 software, and the ratio of emission values was plotted against an *in situ* high potassium-nigericin calibration curve as described (Thomas *et al.*, 1979) to generate absolute values from the ratios. Ten to 30 hermaphrodite nematodes were imaged per experiment.

**Determination of Adenine Nucleotide Concentrations.** AMP and ATP were detected using HPLC. Briefly, 200 L3 nematode worms were hand-picked from NGM plates seeded with OP50 bacteria and transferred to a tube containing 20 μl M9 buffer; 40 μl of 0.4 M perchloric acid was then added to the tube, and the tube was then placed on ice and subjected to sonication using a Branson Ultrasonics (Danbury, CT) 450 sonifier equipped with a microtip three times for 20 s interspersed with 30-s cooling periods on ice. The worms were then neutralized with 4 μl of 4 M potassium perchlorate and centrifuged at 14,000 rpm at 4°C for 2 min. The supernatant was removed and purified through a 0.44-μm syringe filter and immediately run on an LC-20AD liquid chromatograph (Shimadzu Scientific Instruments, Columbia, MD). The nucleotides were separated on a Nova-Pak C18 2 × 150-mm column

at 30°C at a flow rate of 0.4 ml/min (Waters Chromatography, Milford, MA). The mobile phase was comprised of 10 mM  $K_2HPO_4$  and 5 mM tetrabutylammonium hydrogen sulfate. Peaks were identified and concentrations determined from similarly prepared standards.

**Tissue Culture.** Clone 9 cells were in F-12K media (GIBCO, Rockville, MD) containing phenol-red, 2.5% sodium bicarbonate, 10% FBS (Atlanta Biologicals, Norcross, GA), and penicillin/streptomycin. Cells were grown in 100-mm Petri dishes for normal maintenance. Before imaging, cells were diluted and transferred to 12-well tissue culture dishes containing a single 12-mm acid-washed glass coverslip. Cells were allowed to grow for 48–60 h. Cells were then transfected with Scrambled or Opa1 siRNA using oligofectamine (Invitrogen, Carlsbad, CA) or Control or hFis1 overexpression constructs using Lipofectamine LTX (Invitrogen) and allowed to continue growth for 1–2 d before examination. Cells were then treated with MitoTracker Red CMXRos (Invitrogen) to investigate mitochondrial morphology (1 h) or 2,7-bis(carboxyethyl)-5(6)-carboxyfluorescein (BCECF; 15 min) to measure intracellular pH. MitoTracker-stained coverslips were fixed using formaldehyde and mounted in Fluoromount G (Southern Biotechnology Associates, Birmingham, AL) before examination. BCECF-loaded cells were examined under a high NA, 20× air objective on a Nikon Eclipse TE2000-S inverted fluorescent microscope (Melville, NY). Determination of intracellular pH was accomplished using dual-excitation imaging, where two sequential 10-ms exposures were taken at 490 and 440 nm and the emission at 535 nm was measured for each. Ratios were converted to pH using an independently created calibration curve. Image acquisition was accomplished using the instruments described above.

**Confocal Microscopy.** Confocal micrographs were taken on an Olympus IX81 inverted laser scanning confocal microscope (Melville, NY). Images were taken using either the 60× or 100× oil objective (worms) or 100× oil objective (Clone 9 cells). Z-stacks ranging from 5 to 30 slices were taken for each specimen examined. Olympus FluoView1000 software was used to predict optimal slice thickness and for post hoc image processing and analysis. For imaging purposes nematodes were mounted and anesthetized as described above. Clone 9 cells were grown on coverslips and mounted onto glass slides using Fluoromount G.

## RESULTS

**RNAi Screen Reveals a Link between Mitochondria and Cellular pH Homeostasis in the Intestine of *C. elegans*** In an effort to identify gene products necessary for the maintenance of intestinal intracellular pH (pHi) in *C. elegans* we performed a reverse-genetic screen of genes coded for on Chromosome II using double-stranded RNA-mediated gene interference (RNAi). To perform the screen, worms carrying a multicopy extrachromosomal array encoding the pH-sensitive GFP-variant pHluorin driven by the intestine-specific *nhx-2* gene promoter (Nehrke, 2003) were fed bacteria expressing double-stranded RNA using an RNAi library created by J. Ahringer (Fraser *et al.*, 2000; Kamath *et al.*, 2001). The intestinal pHi was measured by ratiometric fluorescent imaging of the pHluorin biosensor in anesthetized worms. The gene *nhx-2* encodes a sodium-proton exchanger in the intestine whose loss causes cellular acidification (Nehrke, 2003; Pfeiffer *et al.*, 2008), and *nhx-2* was used as a positive control for efficacy. The screen resulted in the identification of 40 target genes whose loss reliably reduced the pHi of intestinal cells (Figure 1; Table S1). Not surprisingly given the fact that the nematode intestine is the main fat storage tissue and that catabolic processes likely drive acidification under normal metabolic demand, no gene targets were identified that significantly increased the pHi of the intestinal epithelia (data not shown).

Of the positive target genes, the most abundant class was a group of nine whose gene products were annotated to have a putative or proven mitochondrial function (Figure 1). Eight of these were predicted to function in the mitochondrial electron transport chain (ETC) either directly, as protein subunits of the ETC complexes, or indirectly as components of the dedicated mitochondrial translational machinery. The latter group affects ETC function because of

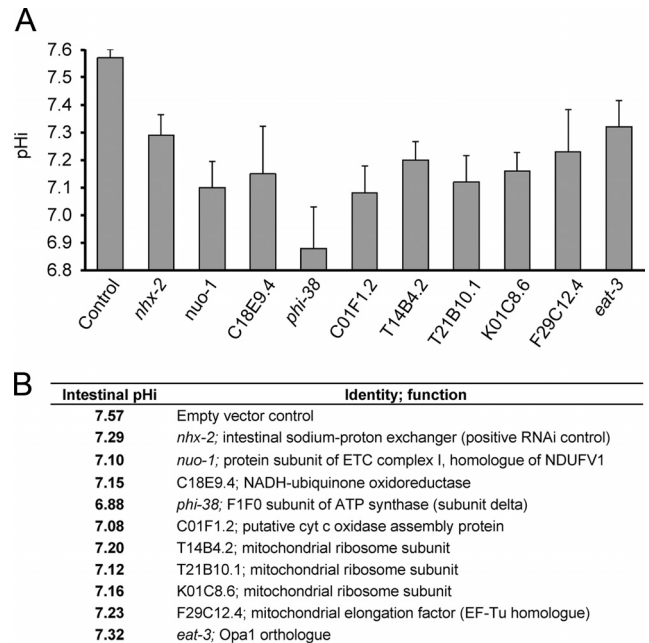


**Figure 1.** RNAi screen of chromosome II identifies nine mitochondrial targets necessary for maintaining normal intestinal intracellular pH. The identification of gene products required for normal regulation of intracellular pH (pHi) in *C. elegans* intestinal cells was accomplished using an established RNAi bacterial feeding library encompassing nearly the entire coding potential of *C. elegans* chromosome II (Geneservice, Cambridge, United Kingdom). (A) Targeting of nine nuclear genes that encode mitochondrial proteins resulted in significant ( $p \leq 0.01$ ) acidosis. The identity of the gene products as shown in B suggested that eight of the nine functioned directly or indirectly in electron transport, with the exception being the inner membrane protein fusion GTPase EAT-3. Empty vector (control) and *nhx-2* RNAi were used as negative and positive controls, respectively. Worms were anesthetized and imaged under glass coverslips as described in *Materials and Methods*. A list of other positive targets can be found in Table S1. Error bars, SEM;  $n = 3$ –5 trials per strain and 15–30 worms per trial.

their necessity in translating the 13 ETC protein subunits encoded by the mitochondrial genome. The fact that these eight targets induced acidification could reasonably be attributed to the fact that the loss of ETC function can cause acidosis, primarily as a result of lactate accumulation, in both worms and humans (Grad and Lemire, 2004). However, the final gene identified was the *C. elegans* orthologue of the mammalian *OPA1* gene, termed *eat-3* in worms, whose product is necessary for fusion of the mitochondrial inner membrane (Kanazawa *et al.*, 2008). Loss of *OPA1* in humans leads to ADOA (Alexander *et al.*, 2000; Deletre *et al.*, 2000), whereas fragmentation of the mitochondrial network and susceptibility to oxidative stress have been associated with *eat-3* mutations in worms (Kanazawa *et al.*, 2008). It is possible that disrupting *eat-3* expression might cause the accumulation of lactate by reducing ETC function, but lactic acidosis has not been noted in ADOA sufferers and, as discussed below, treatments designed to relieve lactic acidosis do not prevent acidification resulting from the loss of *eat-3* (Figure S1).

There is significant potential for cellular acidification to contribute to the etiology of mitochondrial diseases. Although cellular pH is thought to act as a synergistic messenger, providing a metabolic context through which the action of other signals are interpreted (Busa and Nuccitelli, 1984), recent evidence has suggested that pH may play a role

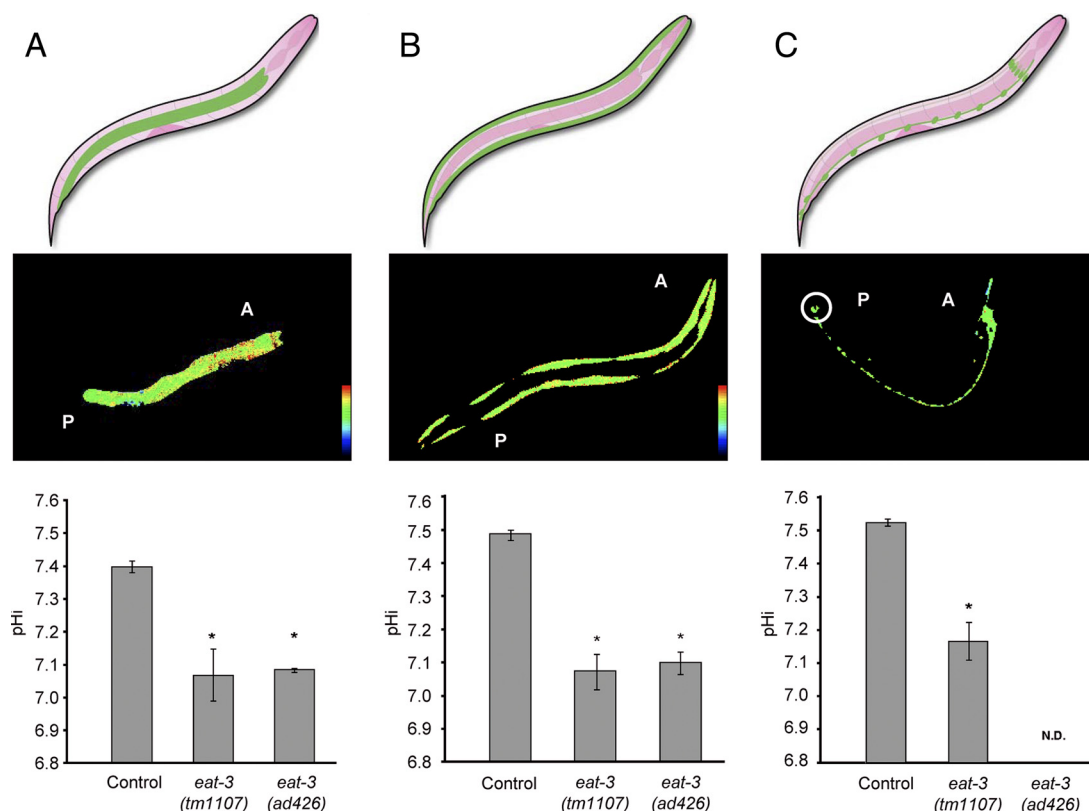


**Figure 2.** Mutations in *eat-3* cause acidification in multiple tissues. Schematic diagrams depicting the expression patterns in green for the pH biosensor transgenes (top), representative pseudocolored ratio maps (alkaline = red > blue = acidic) obtained from fluorescence imaging of the relevant pH biosensors (center), and average pH measurements (bottom) for intestinal cells (A), muscle cells (B), and neurons (C) are shown. The pH values were measured in live unrestrained wild-type (control) and *eat-3* mutant strains using dynamic ratiometric fluorescence imaging as described in *Materials and Methods*. A, anterior; P, posterior. The white circle in the middle panel of C denotes the posterior ganglion, and the pH data were obtained from an ROI encompassing these neurons specifically. Neuronal pH was not measured in the *eat-3(ad426)* mutant. \* $p \leq 0.01$  versus the relevant control. Error bars, SEM;  $n = 3\text{--}5$  trials per strain and 10–30 worms per trial.

in more acute signaling processes, as well (Ludwig *et al.*, 2003; Zha *et al.*, 2006; Beg *et al.*, 2008; Pfeiffer *et al.*, 2008). Thus, acidification is likely to have both indirect and direct effects on cell function. Hence it is intriguing that nearly all of the mitochondrial targets screened through RNAi that result in phenotypic abnormalities are associated with alterations in cellular pH.

**Mutations in *eat-3* Cause Acidification of the Intestine, Muscle Cells, and Neurons** Although RNAi is a useful tool for high-throughput screening, one of the advantages of the worm model is the vast repertoire of existing genetic mutations. To validate our RNAi data, we obtained two strains containing different *eat-3* mutant alleles. The *eat-3(tm1107)* allele, which carries a 417-base pair deletion resulting in a severe truncation of the protein and is likely a null allele, was created by the Japanese National Bioresource Project. The *eat-3(ad426)* allele, which has a point mutation in the GTPase domain resulting in a very strong reduction-of-function (rf), was identified by Leon Avery through an unbiased genetic screen (Avery, 1993). Intestinal pH was measured in these two mutant strains by crossing in a transgene expressing the biosensor pHluorin.

During the course of this work, our laboratory found that intestinal pH oscillates during and contributes to the rhythmic nematode defecation behavior, resulting in cellular acidification occurring every ~45 s (Beg *et al.*, 2008; Pfeiffer *et al.*, 2008). To incorporate this finding into our experimental

paradigm, we turned to dynamic pH imaging in freely moving, unanesthetized worms. The intestinal pH was extracted from dynamic traces such as those shown in Supplemental Figure S2 at 25 s after pBoc, which is the first motor step in defecation, and our data are thus time-normalized relative to the pH oscillations and the defecation behavior. In this freely moving model, we found that both the *eat-3(ad426)* and *(tm1107)* mutants demonstrated significant acidification of the intestinal cytoplasm relative to the wild-type control (Figure 2A). These differences persisted through the entire defecation cycle and became even more pronounced as a function of age (Figure S2). The absolute values reported in Figures 1 and 2 likely reflect the data acquisition method and may not be directly comparable; freshly anesthetized worms generally exhibit intestinal pH values that are near the peak of the traces obtained with freely moving worms. Nevertheless, similar extents of acidification are observed using both techniques.

Although the intestinal cells of the *C. elegans* exhibit rhythmic pH oscillations, this is not the case for the majority of eukaryotic cell types. Therefore, we had to consider the possibility that the acidification observed in the *eat-3* mutants was dependent on these pH oscillations. To address this concern, we examined two other tissues where the pH does not rhythmically oscillate (K. Nehrke, personal observations), the body wall muscles and the neurons. Expression of the biosensor pHluorin was driven by the neuron- and

**Table 1.** Cellular pH in morphology mutants

Genotype	Intestine	Muscle	Neuron
Control	7.40 ± 0.02*	7.49 ± 0.02*	7.52 ± 0.01*
<i>eat-3(ad426)</i>	7.09 ± 0.01*	7.10 ± 0.03*	N.D.
<i>eat-3(tm1107)</i>	7.07 ± 0.07*	7.07 ± 0.05*	7.17 ± 0.06*
<i>eat-3(tm1107)</i> <i>rnyEx079</i>	N.D.	7.38 ± 0.02*	N.D.
<i>fzo-1(tm1133)</i>	7.09 ± 0.02*	7.32 ± 0.03*	7.34 ± 0.02*
<i>eat-3(ad426);</i> <i>drp-1(cq5)</i>	7.36 ± 0.02*	7.46 ± 0.02*	N.D.
<i>drp-1(tm1108)</i>	7.41 ± 0.03*	7.54 ± 0.03*	N.D.

All measurements were made in live, freely moving worms. Because intestinal pH oscillates during a rhythmic behavior, for this tissue pH was time-normalized to 25 s after pBoc, the first motor component of the behavior. The *rnyEx079* array encodes a genomic *eat-3* rescue fragment and a muscle pH biosensor.

\*  $p < 0.01$  vs. the control; mean ± SEM;  $n = 3-5$  trials per strain with 15–30 worms per trial. N.D., not determined.

muscle-specific *cah-4a* and *myo-3* gene promoters, respectively, as shown in the top panels of Figure 2, and dynamic imaging was performed in freely moving worms. Our data demonstrate that these diverse cell types become acidified in *eat-3* mutants to a similar extent as the intestine (Figure 2B and 2C; Table 1), confirming that acidification is not dependent upon oscillatory pH signaling.

Finally, a hallmark of many mitochondrial diseases such as Leigh's syndrome is the chronic accumulation of lactate, which is clinically diagnosed as lactic acidosis. One source of lactic acidosis in Leigh's can be mutations in the electron transport chain NDU6 subunit of Complex I, and RNAi of *nuo-1*, the worm ortholog of NDU6, results in acidosis in our hands, as well (Figure 1). In fact, when human disease-causing mutations are introduced into the worm NUO-1, they cause a pathological accumulation of lactate that can be reversed by growing the mutants on plates supplemented with sodium dichloroacetate (DCA), a stimulator of pyruvate dehydrogenase (Grad and Lemire, 2004). However, while phenotypic variability is a hallmark of ADOA, this is considered to be an indirect effect of modifiers, as mutations in OPA-1 can lead to mitochondrial DNA instability. However, lactic acidosis is not associated with OPA-1 mutations themselves. To test whether the acidification seen in the *eat-3* mutants might result from lactic acidosis we compared the pH of muscle cells in *eat-3(ad426)* worms grown in the presence or absence of DCA. There was no significant change of muscle cell pH in *eat-3(ad426)* worms treated with DCA, whereas worms where *nuo-1* expression had been targeted using RNAi (Figure 1) exhibited a small but significant recovery in the presence of DCA (Figure S1A). This recovery was even more notable in the intestinal cells compared with muscle (Figure S1B), which may relate to the efficiency of DCA uptake and dispersion through the body. Again, however, the *eat-3(ad426)* mutant did not exhibit any recovery (Figure S1B). Interestingly, DCA treatment suppressed the sickliness that was apparent in *nuo-1(RNAi)* worms, as has been reported previously (Grad and Lemire, 2004), but had little effect on the *eat-3(ad426)* mutants, which have been described as "generally disgusting" (L. Avery, WormBase; www.wormbase.org/db/gene/gene?name=WBGene00001134; Class=Gene).

**Mitochondrial Fragmentation Is Responsible for Acidosis**  
We further considered the idea that acidification may not

result from mitochondrial fragmentation per se but instead be caused by the loss of the *eat-3* gene product acting in an unrelated capacity. To test this idea, we turned to a suppressor mutation in the profission dynamin-related GTPase gene *drp-1* that restores mitochondrial morphology in an *eat-3(ad426)* mutant (Kanazawa *et al.*, 2008). This *eat-3(ad426); drp-1(cq5)* double mutant was generously provided by Dr. A. van der Bliek. Notably, *cq5* only suppresses *ad426*, but not *tm1107*, which is the *eat-3* null allele, suggesting that the balance between mitochondrial fission and fusion determines morphology. Therefore, reducing fission through the *cq5* mutation is only effective if the capacity exists for fusion to occur, even if at reduced levels. Inasmuch as the pH in the muscle cells of the double *cq5/ad426* mutant is not significantly different from that of the control worms (Table 1), acidification is likely not the result of losing a secondary activity, but is directly related to EAT-3 regulation of mitochondrial morphology.

As a parallel approach we examined the role of the nematode Mfn ortholog FZO-1 in cellular pH homeostasis. The mitofusins are outer membrane GTPases that are required for mitochondrial fusion. The *fzo-1* gene encodes the single mitofusin orthologue in *C. elegans*. The *fzo-1(tm1133)* allele is a 419-base pair deletion with a 14-base pair insertion and is likely null, and the loss of FZO-1 causes mitochondrial fragmentation in worms (Breckenridge *et al.*, 2003; Ichishita *et al.*, 2008; Tan *et al.*, 2008; Figure 3). Transgenes coding for pHluorin were crossed into the *fzo-1(tm1133)* mutant strain, and pH was measured by recapitulating the approach used to examine the *eat-3* mutants. Our results demonstrate that the loss of FZO-1 is sufficient to significantly reduce pH in the intestine, muscle cells, and neurons (Figure S2; Table 1). We note that although the *fzo-1* gene is found on Chromosome II, it did not show up in our first-pass RNAi screen, and thus falls into the false-negative category; subsequent RNAi targeting using the library clone was also ineffective at reducing *fzo-1* expression (data not shown). However, the *fzo-1(tm1133)* mutation is nonadditive to *eat-3* RNAi with respect to pH homeostasis (Figure S3), consistent with the observation that the loss of either FZO-1 or EAT-3 causes mitochondrial fragmentation. Thus, fragmentation itself is sufficient to cause intracellular acidosis. However, the converse is not true: a loss of fission through mutation of the dynamin-related protein *drp-1* does not influence cellular pH (Table 1).

Unlike in the *eat-3* mutants, the extent of acidification observed in the *fzo-1(tm1133)* mutant worms was remarkably different depending on the tissue examined. The intestine of *fzo-1(tm1133)* worms was severely acidified, but muscles and neurons were less impacted (Table 1). Interestingly, this correlated extremely well with the phenotypes of the two mitochondrial fusion mutants. Behavioral measures such as thrashing rate in liquid and the rate of pharyngeal pumping, which correlate well with degenerative changes and reflect viability or health, suggested that the *fzo-1(tm1133)* mutants have a comparatively mild phenotype (Figure 4). The difference in phenotype could be readily seen in Normarski images, which illustrate the severe and mild reduction in body size associated with *eat-3* and *fzo-1* mutations, respectively (Figure 4A). Furthermore, Oil-Red-O staining showed that the loss of mitochondrial fusion resulted in marked decrease in global fat mass, but again, the reduction was more pronounced in the *eat-3(tm1107)* mutants (Figure 4B).

The introduction of an extrachromosomal array containing a genomic *eat-3* fragment into the *tm1107* mutant background was sufficient to rescue its phenotypic deficits (Fig-

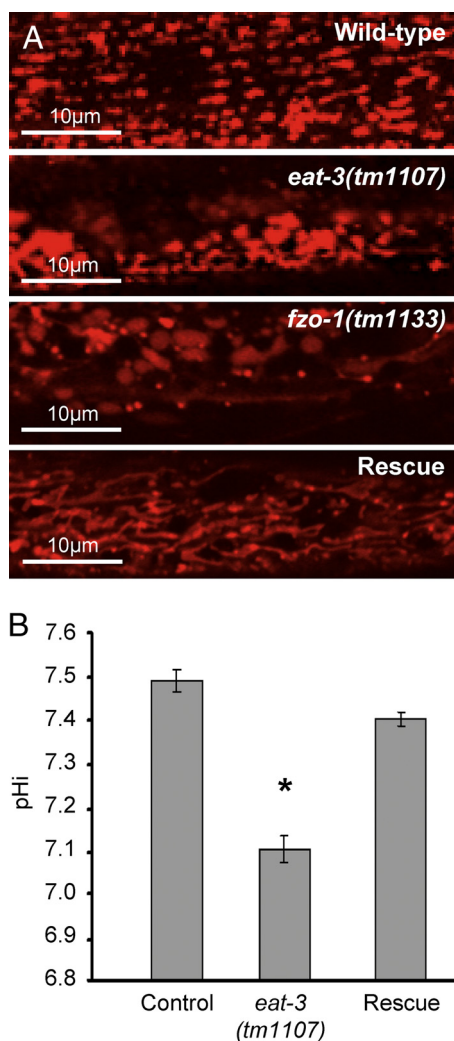


**Figure 3.** An *eat-3* genomic fragment rescues muscle pH<sub>i</sub> and mitochondrial morphology in the *eat-3(tm1107)* mutant background. Confocal images of mitochondria in the body-wall muscle of wild-type (control), *eat-3(tm1107)*, *fzo-1(tm1133)*, and rescued *eat-3(tm1107)* mutant worms (rescue). (A) Mitochondria were labeled with MitoTracker Red CMXRos. Specific labeling of the mitochondria was confirmed by colabeling experiments using a mitochondrial targeted GFP (Figure S4). Images shown are of single z-slices from a confocal stack obtained using a 100× objective and optimal slice thickness. (B) Muscle pH<sub>i</sub> in the rescued *eat-3(tm1107)* strain. pH measurements were made in freely moving worms. Control measurements were taken from a wild-type worm expressing the same combination of transgenes as the rescued *tm1107* mutant. Error bars, SEM; n = 3–5 trials per strain and 10–30 worms per trial. \*p ≤ 0.01 versus control.

ure 4). We also assessed the effect of the rescue array on pH<sub>i</sub> and mitochondrial morphology. To measure muscle pH<sub>i</sub> in the rescued line, the array also contained a *Pmyo-3::pHluorin* transgene (*Materials and Methods*). However, because of spectral overlap with GFP, we were unable to use a genetically encoded marker to tag mitochondria and simultaneously examine morphology and pH<sub>i</sub> in the rescued strain. We considered using red fluorescent proteins to label the mitochondria, as they do not exhibit spectral overlap with pHluorin, but they also tend to aggregate. However, the mitochondrial dye MitoTracker Red CMX-Ros is spectrally distinct from pHluorin and labels mitochondria uniformly.

The disadvantage is that it also labels mitochondria indiscriminately. To visualize muscle mitochondria specifically a single confocal slice was examined from stained worms; colabeling experiments using a genetic marker to tag muscle mitochondria indicated a nearly complete overlap with dye-stained structures in the muscle cells (Figure S4). Using these approaches, we determined that the rescue was associated with reduced mitochondrial fragmentation (Figure 3A) and restored muscle pH<sub>i</sub> to near-normal values (Figure 3B). However, the mitochondria in the rescued strain appeared to be more fused relative to the wild-type controls, and the worms themselves exhibited a somewhat larger body size. These observations are consistent with the notion that the transgenic overexpression of *eat-3*, like overexpression of *fzo-1* (Tan *et al.*, 2008), may have a dominant effect on morphology.

**Mitochondrial Redox Status Is Altered in *eat-3(ad426)* Fusion Defective Mutants** Despite significant focus, there remains some uncertainty as to the effect of fragmentation on mitochondrial function and cellular metabolism. For example, it has been suggested that the loss of mitochondrial fusion reduces oxidative phosphorylation and causes dissipation of membrane potential in mammalian cells (Chen *et al.*, 2005). However, global ATP levels remain unchanged under standard growth conditions in both mutant Opa1 and Mfn2 cell lines, likely indicating a switch to alternative means of energy production (Baloh *et al.*, 2007; Zanna *et al.*, 2008). These considerations prompted us to explore several physiological measures related to mitochondrial function, including redox status of the matrix and AMP/ATP ratios in the mutant worms.

To measure redox status, a body wall muscle-specific promoter (*Pmyo-3*) was used to express a mitochondrial matrix targeted redox-sensitive GFP (mito-roGFP1; Hanson *et al.*, 2004). Confocal reconstruction using mito-roGFP1-labeling demonstrated severe fragmentation of the mitochondrial network in both the *eat-3(tm1107)* and *fzo-1(tm1133)* loss-of-function mutants (Figure 5A). These results mirrored those obtained using Mitotracker CMX-Ros labeling (Figure 3). Interestingly, the *fzo-1(tm1133)* mitochondria appeared to be more fragmented, possibly because FZO-1 is required for outer membrane fusion, whereas the loss of the inner membrane GTPase EAT-3 allows small amounts of residual outer membrane fusion to occur (Meeusen *et al.*, 2006; Song *et al.*, 2009). This is consistent with electron tomography of mitochondria from *eat-3* mutant worms, demonstrating what appears to be pinched-off vacuoles residing in the matrix; these vacuoles are not observed in *fzo-1(tm1133)* mutants (Kanazawa *et al.*, 2008).

There was also a dramatic difference between the mitochondrial redox status in the *eat-3(ad426)* and *fzo-1(tm1133)* mutants. Although the *fzo-1(tm1133)* mutant displayed no appreciable change in the mitochondrial redox potential of muscle cells compared with wild-type controls, the *eat-3(ad426)* mutants displayed a sharp shift toward a more oxidized environment (Figure 5B). This seemingly small shift could reflect relatively large changes in the production of transient reactive oxygen species (ROS), which have a very limited half-life and may be extremely relevant to cellular function. Parallel experiments measuring mitochondrial redox status in the intestine demonstrated that the loss of EAT-3, but not FZO-1, led to a shift toward oxidation in these cells, as well (Figure S5). It is likely that the loss of *eat-3* has functional consequences at the inner membrane, where the molecular components of the ETC reside. These data may also help to explain previous reports regarding the

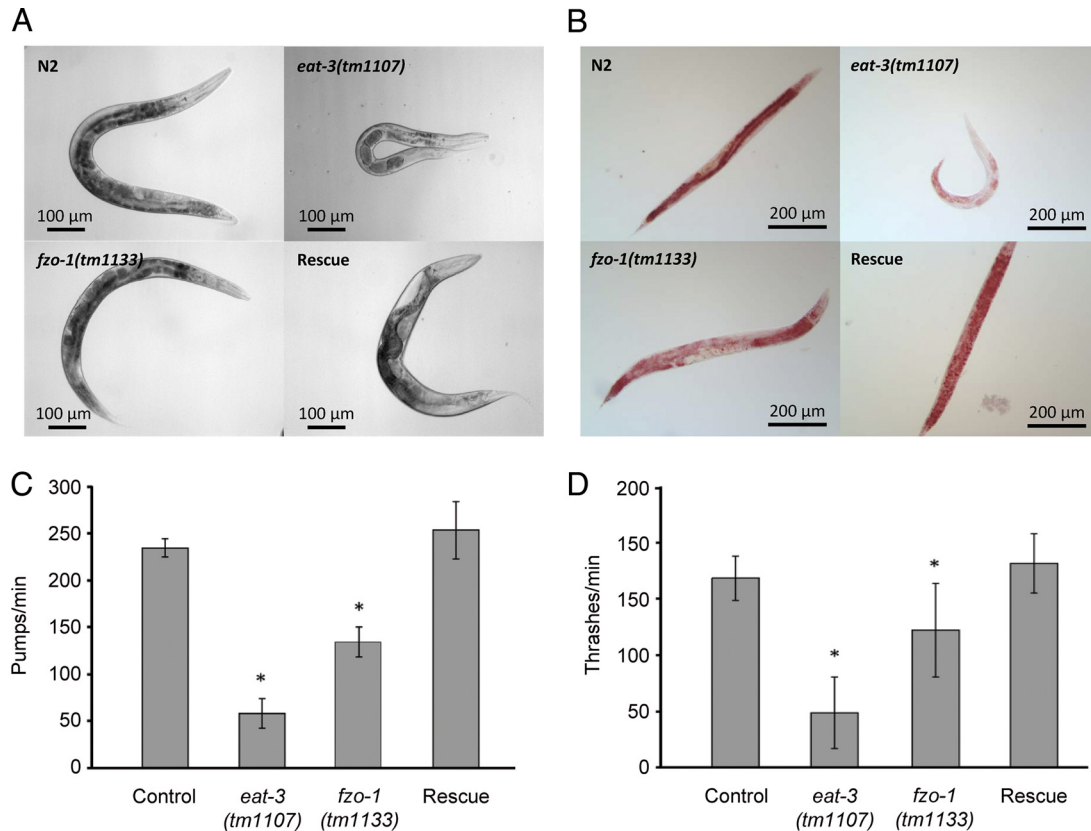


**Figure 4.** *eat-3* and *fzo-1* mutant worms have distinct phenotypes. Phenotypic parameters were assessed in control worms, *eat-3(tm1107)*, and *fzo-1(tm1133)* deletion mutants, and an *eat-3(tm1107)* background expressing the genomic rescue fragment (rescue), as indicated. (A) Brightfield images illustrating the reduction of body size that occurs in the *eat-3(tm1107)* mutant, and (B) the reduction in total fat mass as determined by Oil-Red-O staining. (C) The rate of pharyngeal pumping and (D) thrashing upon immersion in liquid (M9) were reduced in both the *eat-3(tm1107)* and *fzo-1(tm1133)* deletion mutants. In all of these cases, expression of the genomic rescue fragment suppressed the phenotype. \* $p \leq 0.01$  versus control. Error bars, SEM;  $n = 5$  (pumping) or 6–8 (thrashing) trials.

increased sensitivity of *eat-3* mutants, but not *fzo-1* mutants to oxidative stress (Kanazawa *et al.*, 2008).

Further evidence suggesting oxidative signaling as a mechanistic component of *eat-3* mutation-induced acidification was seen when fusion-defective worms were grown in the presence of the antioxidant *N*-acetylcysteine (NAC). Supplementation with NAC caused a small but statistically significant suppression of acidosis in the *eat-3* mutant, but not the *fzo-1* mutant or control worms (Figure S6A). In agreement with oxidative signaling leading to acidification, we further found that *eat-3* RNAi-induced acidification could be suppressed by overexpression of the ROS scavenger protein catalase (Figure S6B). Finally, in contrast to *eat-3*, the *fzo-1* mutant was essentially unresponsive to NAC, but acidosis could be suppressed by DCA supplementation (Figure S6C), suggesting that lactate accumulation may occur in this mutant strain. These data indicate that the mechanism leading to acidification differs between the *eat-3* and *fzo-1* mutants, despite the fact that both cause fragmentation of the mitochondria.

Many of the metabolic pathways that sense global energy levels in both worms and mammals respond to AMP/ATP ratios rather than bulk ATP itself, and alternative mechanisms for ATP production such as glycolysis can be triggered under conditions of energy starvation or hypoxia (Salt *et al.*, 1998; Hardie *et al.*, 1999; Marsin *et al.*, 2000; Marsin *et al.*, 2002; Apfeld *et al.*, 2004). Therefore, we examined energy charge in control and fusion defective mutant worm popu-

lations via HPLC detection of AMP and ATP in whole worm extracts as previously described (Apfeld *et al.*, 2004). Our results indicate that in both *fzo-1* and *eat-3* mutants the AMP/ATP ratio is not significantly altered in comparison to controls, demonstrating that global energy production is not disrupted in these mutants (Table 2). Further work will be needed to determine if the mitochondria in the *eat-3* mutants are defective in energy production and if so, whether up-regulation of alternative energy pathways occurs as a compensatory mechanism.

**Mitochondrial Fragmentation Results in Acidification of Mammalian Cells** Our work in worms led to the idea that cellular acidification may contribute to the etiology of mitochondrial diseases in man. To test this idea, we induced mitochondrial fragmentation in cultured mammalian Clone 9 (epithelial rat liver) cells and measured their cellular pH. Fragmentation was induced either by transfection of a vector driving the recombinant overexpression of the pro-fusion protein hFis1 (a kind gift from Dr. Y. Yoon) or by siRNA knockdown of the pro-fusion protein Opa1, analogous to the *eat-3(RNAi)* treatment in worms. Confocal micrographs of mitochondria stained with MitoTracker Red CMX-Ros revealed that both of these treatments were sufficient to fragment the mitochondrial network in the mammalian cell line (Figure 6, A–C). The pH-sensitive vital dye BCECF was used to measure the pH of cells overexpressing hFis1 or transfected with either control or Opa1-targeted siRNA. The re-

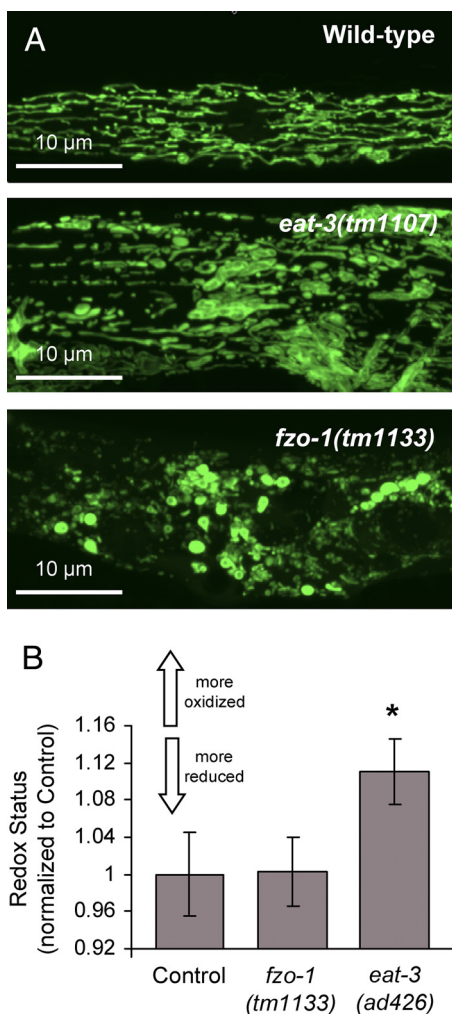


**Figure 5.** The loss of EAT-3, but not FZO-1 alters mitochondrial redox potential. Mitochondrial redox status was measured in wild-type (control), *eat-3(ad426)*, and *fzo-1(tm1133)* worms as described in *Materials and Methods* using the mitochondrial redox-sensitive GFP (mito-roGFP2) probe targeted to the mitochondrial matrix of body wall muscle cells. (A) Expression pattern of the mito-roGFP1 in the body wall muscle of wild-type, *eat-3(ad426)*, and *fzo-1(tm1133)* mutant worms. Images are confocal micrographs comprised of 25–35 individual z-slices. (B) A mutation in *eat-3* causes the redox status as measured by the ratio of emissions at 535 nm (after dual excitation at 410 and 470 nm) to increase relative to controls, which is indicative of a more oxidized mitochondrial environment. \* $p \leq 0.01$  versus control. Error bars, SEM;  $n = 3$ –5 trials per strain and 10–30 worms per trial.

sults in Figure 6D indicate that either method of fragmenting the mitochondrial network results in significant acidification of the cytosol compared with control cells transfected with a scrambled siRNA (or empty vector; data not shown). This suggests that acidification could be a contributing factor to cellular dysfunction in morphology diseases such as ADOA.

## DISCUSSION

Although the dynamic nature of mitochondria was established several decades ago, only recently have we begun to understand the importance of this behavior to cellular function and organism viability. Our data have revealed a novel

**Table 2.** AMP/ATP ratio in morphology mutants

Genotype	AMP/ATP ratio	p
Control	0.07 ± 0.03	NA
<i>eat-3(tm1107)</i>	0.04 ± 0.03	0.16
<i>fzo-1(tm1133)</i>	0.09 ± 0.06	0.82
<i>eat-3(tm1107) rnyEx079</i>	0.07 ± 0.02	0.94

Adenine nucleotide concentrations in whole worm extracts were detected using HPLC as described in *Materials and Methods*. Each trial included ~200 L4 larval worms. Values are mean ± SD, Student's *t* test compared with control;  $n = 4$ . The rnyEx079 array encodes a genomic *eat-3* rescue fragment and a muscle pH biosensor.

role for mitochondrial dynamics in intracellular pH homeostasis that is conserved between nematodes and mammalian cells. We have demonstrated that the predominance of mitochondrial fission over fusion mediated by the functional loss of profusion proteins in both nematode and mammalian models or the overexpression of the profusion protein hFis1 in mammalian cell culture results in significant cellular acidification. Interestingly, the loss of mitochondrial fission leading to high levels of mitochondrial interconnectivity has no significant effect on pHi in the nematode model indicating that the phenomenon is unidirectional (Table 1).

The list of human disorders associated with disrupted mitochondrial dynamics is steadily increasing (for review see Chen and Chan, 2009), but the exact nature of the link between mutation and disease remains to be discovered. Our data provide another piece to the increasingly complex puzzle relating mitochondrial structure to organelle function and cellular homeostasis. For example, there is undeniable evidence that acidification has functional consequences on nearly every aspect of cell physiology and can contribute to the pathophysiologic mechanisms of cellular dysfunction and death, as well.

So, if acidification contributes to the pathogenesis of mitochondrial morphology diseases, why is a common feature of this class of disease that they manifest predominantly in neuronal tissues? After all, mutations in genes that regulate structural dynamics affect mitochondrial architecture throughout the body. Could it be that neurons are particularly susceptible to acidosis? Interestingly, it has been shown that neuronal NMDA and AMPA receptors, as well as voltage-dependent calcium channels, are exquisitely sensitive to pH (Giffard *et al.*, 1990; Ou-Yang *et al.*, 1994; Kiss and Korn, 1999; Ihle and Patneau, 2000; Shah *et al.*, 2001). As might be extrapolated from these observations, neurons that are exposed to acidic environments or experience intracellular acidification are defective in several aspects of ion transport and cellular signaling, and the sensitivities of these receptors/channels to pH can lead to the accumulation of cytosolic  $Ca^{2+}$ , which can contribute to apoptotic cell death or excitotoxicity (McDonald *et al.*, 1998; Ying *et al.*, 1999; Xiong *et al.*, 2004). In addition, mitochondria routinely undergo regulated fission and fusion in neurons in order to be transported along microtubules to the synaptic bouton, where energy demand is greatest (Li *et al.*, 2004; Verstreken *et al.*, 2005; Chen *et al.*, 2007). Taken together it is not unreasonable to hypothesize that acidification as a result of being unable to reassemble mitochondria after transport could serve as a molecular basis for the tissue-specific degradation seen in diseases such as CMT2A and ADOA (Carelli *et al.*, 2009). In support of a role for acidification in the disease

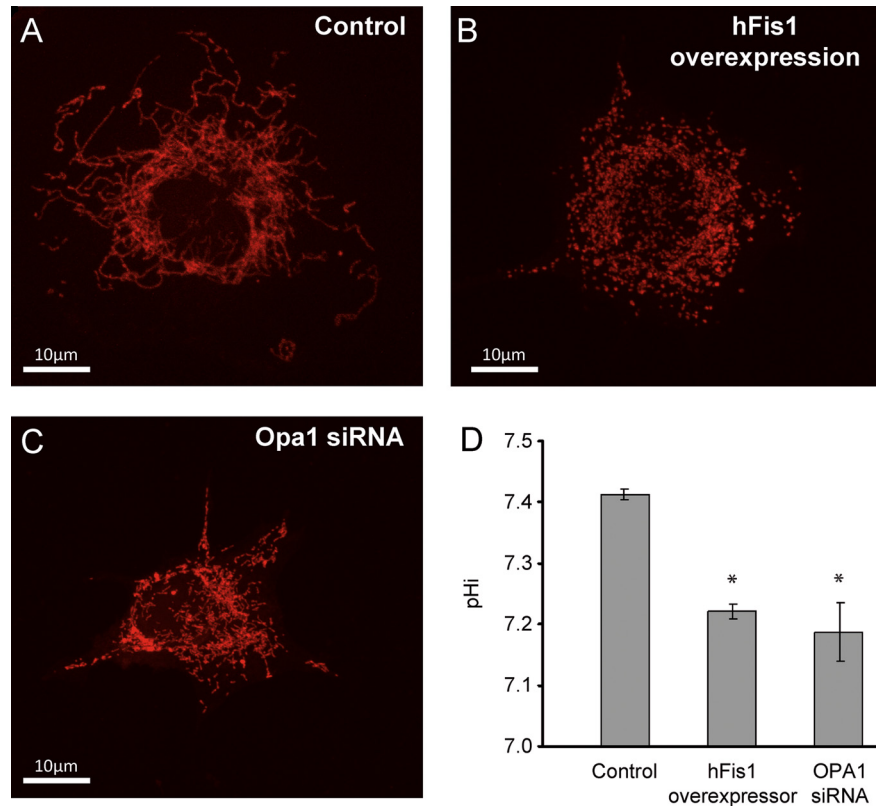


**Figure 6.** Fragmentation of the mitochondrial network in cultured mammalian cells causes cellular acidification. Confocal images of MitoTracker Red CMXRos-labeled mitochondria in cultured Clone 9 cells (A) treated with control (scrambled) siRNA, (B) transfected with hFis1 cDNA, or (C) treated with Opa1 siRNA. (D) The pHi of cultured Clone 9 (rat liver) cells was measured using the pH-sensitive dye BCECF using dual-excitation ratiometric fluorescent imaging. Mitochondrial fragmentation was induced by the overexpression of myc-tagged hFis1 or siRNA targeting of Opa1, as indicated. \* $p \leq 0.01$  versus control. Error bars, SEM;  $n = 3$  trials of 10 cells each.

etiology, we have shown that pHi reflects the severity of the mutant phenotype in *C. elegans*; we hypothesize that ability of mutant worms to survive at all reflects the fact that the neuronal processes in worms are relatively short. It remains to be seen whether genetic manipulations designed to disrupt neuronal pH homeostasis has the capacity to recapitulate the *eat-3* mutant phenotype, but it is intriguing that a knockout of the global housekeeping  $\text{Na}^+/\text{H}^+$  exchanger *NHE1* has as its most apparent consequence a tendency toward epileptic seizures (Bell *et al.*, 1999).

We have also considered whether changes in mitochondrial morphology actively trigger cellular acidification or whether acidification is an indirect consequence of shifting metabolic pathways to satisfy energy demand. Previous reports have linked *OPA1* mutations to decreased mitochondrial energy production (Chen *et al.*, 2005; Zanna *et al.*, 2008). A reduced efficiency of ATP synthesis may reflect respiratory uncoupling resulting from proton leak or electrical slip (Dominique *et al.*, 2007; Arnaud *et al.*, 2008), and increased expression of the adenine nucleotide transporter ANT1 has been found in fibroblasts from CMT2A patients (Guillet *et al.*, 2010). However, recent evidence from a study of related ADOA sufferers carrying a novel mutation in the GTPase domain of OPA1 has revealed that the disease can occur in the absence of altered energy production (Spinazzi *et al.*, 2008). Moreover, our data demonstrate that AMP/ATP levels, which are tightly regulated and conserved in both mammals and worms, in both *eat-3* and *fzo-1* morphology mutants are similar to wild-type controls. This is in general agreement with the idea that metabolic deficits may contribute to the disease etiology, but are not the central cause.

So, how might fragmentation cause acidification? The trigger for both apoptosis and necrosis includes a transient cellular acidification that may be important for caspase ac-

tivation (Li and Eastman, 1995; Matsuyama *et al.*, 2000; Syntichaki *et al.*, 2005). This acidification has been suggested to result from reversal of the mitochondrial F1F0 ATPase. However, a reversal of the ATPase, encoded by the *phi-38* gene in worms, is unlikely to result in the acidification observed in the morphology mutants. RNAi of *phi-38* on its own causes acidification (Table 1) and fails to suppress acidification in the *eat-3* mutant (data not shown), whereas the mitochondrial pH becomes more acidic after loss of *eat-3* (D. Johnson and K. Nehrke, unpublished data). This is the opposite of what would be expected if the ATPase were burning ATP to pump protons into the cytoplasm. It is also important to note that mitochondrial fragmentation in the worm model does not lead to excess apoptosis (Kanazawa *et al.*, 2008), suggesting that acidosis is necessary but not sufficient to trigger cell death.

Our data suggest that distinct mechanisms lead to acidosis in the two fusion mutants. Considering the ability of DCA to suppress acidosis in the *fzo-1* mutant, a metabolic switch to glycolysis is likely resulting in the buildup of lactate. However, we have found that DCA does not suppress acidification in the *eat-3* mutant. Instead, we find that reducing agents such as NAC, or overexpression of the ROS scavenger protein catalase, can suppress acidification (Figure S6). Thus, we hypothesize that the mechanistic link in the *eat-3* mutant is ROS, which are a byproduct of mitochondrial respiration and have been well documented to influence the membrane transporters that control pH homeostasis (Wu *et al.*, 1996; Tsai *et al.*, 1997; Hu *et al.*, 1998). The application of oxidizing compounds to cells can also result in acidification (Kaufman *et al.*, 1993; Nakamura *et al.*, 2006). In this context, the oxidized matrix (Figure 5) and the increased susceptibility to oxidative stress (Kanazawa *et al.*, 2008) observed in the *eat-3(tm1107)* mutant may reflect ROS production, which

would correlate well with the severe acidification in muscle and intestinal cells (Table 1) and pronounced phenotype (Figure 4). Although the exact mechanism underlying the cause of the acidification in mitochondrial fusion mutants remains unclear, our findings certainly provide new insight into the pathology and perhaps the cell specificity of diseases caused by altered mitochondrial dynamics.

## ACKNOWLEDGMENTS

We acknowledge the *C. elegans* Gene Knockout Consortium, the *C. elegans* Genetic Center, the Japanese Bioresource Project, Dr. David Gems and Dr. Alex Van der Bliek for strains, and also Dr. Yisang Yoon for the hFis1 overexpression construct and antibody. We also thank Andrew Wojtovich and Dr. Paul Brookes for technical assistance with HPLC measurements of adenine nucleotides. Finally, we thank both Teresa Sherman and Alex Bickel for expert technical assistance. This work was supported in part by Public Health Service Grant R01 HL080810 and National Science Foundation Grant IOS-0919848 (K.N.). D.J. was supported by the Ruth L. Kirschstein National Research Service Institutional Training Grant T32 GM068411 and the Ruth L. Kirschstein NRSA Pre-Doctoral Fellowship F31 GM084506.

## REFERENCES

- Alexander, C., *et al.* (2000). OPA1, encoding a dynamin-related GTPase, is mutated in autosomal dominant optic atrophy linked to chromosome 3q28. *Nat. Genet.* 26, 211–215.
- Apfeld, J., O'Connor, G., McDonagh, T., DiStefano, P. S., and Curtis, R. (2004). The AMP-activated protein kinase AAK-2 links energy levels and insulin-like signals to lifespan in *C. elegans*. *Genes Dev.* 18, 3004–3009.
- Arnaud, C., *et al.* (2008). Hereditary optic neuropathies share a common mitochondrial coupling defect. *Ann. Neurol.* 63, 794–798.
- Avery, L. (1993). The genetics of feeding in *Caenorhabditis elegans*. *Genetics* 133, 897–917.
- Baloh, R. H., Schmidt, R. E., Pestronk, A., and Milbrandt, J. (2007). Altered axonal mitochondrial transport in the pathogenesis of Charcot-Marie-Tooth disease from mitofusin 2 mutations. *J. Neurosci.* 27, 422–430.
- Beg, A. A., Ernstrom, G. G., Nix, P., Davis, M. W., and Jorgensen, E. M. (2008). Protons act as a transmitter for muscle contraction in *C. elegans*. *Cell* 132, 149–160.
- Bell, S. M., Schreiner, C. M., Schultheis, P. J., Miller, M. L., Evans, R. L., Vorhees, C. V., Shull, G. E., and Scott, W. J. (1999). Targeted disruption of the murine Nhe1 locus induces ataxia, growth retardation, and seizures. *Am. J. Physiol.* 276, C788–C795.
- Benard, G., Bellance, N., James, D., Parrone, P., Fernandez, H., Letellier, T., and Rossignol, R. (2007). Mitochondrial bioenergetics and structural network organization. *J. Cell Sci.* 120, 838–848.
- Breckenridge, D. G., Stojanovic, M., Marcellus, R. C., and Shore, G. C. (2003). Caspase cleavage product of BAP31 induces mitochondrial fission through endoplasmic reticulum calcium signals, enhancing cytochrome c release to the cytosol. *J. Cell Biol.* 160, 1115–1127.
- Brenner, S. (1974). The genetics of *Caenorhabditis elegans*. *Genetics* 77, 71–94.
- Busa, W. B., and Nuccitelli, R. (1984). Metabolic regulation via intracellular pH. *Am. J. Physiol. Regul. Integr. Comp. Physiol.* 246, R409–R438.
- Carelli, V., La Morgia, C., Valentino, M. L., Barboni, P., Ross-Cisneros, F. N., and Sadun, A. A. (2009). Retinal ganglion cell neurodegeneration in mitochondrial inherited disorders. *Biochim. Biophys. Acta* 1787, 518–528.
- Chen, H., and Chan, D. C. (2009). Mitochondrial dynamics—fusion, fission, movement, and mitophagy—in neurodegenerative diseases. *Hum. Mol. Genet.* 18, R169–R176.
- Chen, H., Chomyn, A., and Chan, D. C. (2005). Disruption of fusion results in mitochondrial heterogeneity and dysfunction. *J. Biol. Chem.* 280, 26185–26192.
- Chen, H., McCaffery, J. M., and Chan, D. C. (2007). Mitochondrial fusion protects against neurodegeneration in the cerebellum. *Cell* 130, 548–562.
- Davies, V. J., Hollins, A. J., Piechota, M. J., Yip, W., Davies, J. R., White, K. E., Nicols, P. P., Boulton, M. E., and Votruba, M. (2007). Opa1 deficiency in a mouse model of autosomal dominant optic atrophy impairs mitochondrial morphology, optic nerve structure and visual function. *Hum. Mol. Genet.* 16, 1307–1318.
- Delettre, C., *et al.* (2000). Nuclear gene OPA1, encoding a mitochondrial dynamin-related protein, is mutated in dominant optic atrophy. *Nat. Genet.* 26, 207–210.
- Dominique, L., *et al.* (2007). Mitochondrial coupling defect in Charcot-Marie-Tooth type 2A disease. *Ann. Neurol.* 61, 315–323.
- Doonan, R., McElwee, J. J., Matthijssens, F., Walker, G. A., Houthoofd, K., Back, P., Matscheski, A., Vanfleteren, J. R., and Gems, D. (2008). Against the oxidative damage theory of aging: superoxide dismutases protect against oxidative stress but have little or no effect on life span in *Caenorhabditis elegans*. *Genes Dev.* 22, 3236–3241.
- Fraser, A. G., Kamath, R. S., Zipperlen, P., Martinez-Campos, M., Sohrmann, M., and Ahringer, J. (2000). Functional genomic analysis of *C. elegans* chromosome I by systematic RNA interference. *Nature* 408, 325–330.
- Giffard, R. G., Monyer, H., Christine, C. W., and Choi, D. W. (1990). Acidosis reduces NMDA receptor activation, glutamate neurotoxicity, and oxygen-glucose deprivation neuronal injury in cortical cultures. *Brain Res.* 506, 339–342.
- Grad, L. I., and Lemire, B. D. (2004). Mitochondrial complex I mutations in *Caenorhabditis elegans* produce cytochrome c oxidase deficiency, oxidative stress and vitamin-responsive lactic acidosis. *Hum. Mol. Genet.* 13, 303–314.
- Guillet, V., *et al.* (2010). Adenine nucleotide translocase is involved in a mitochondrial coupling defect in MFN2-related Charcot-Marie-Tooth type 2A disease. *Neurogenetics* 11, 127–133.
- Hales, K. G., and Fuller, M. T. (1997). Developmentally regulated mitochondrial fusion mediated by a conserved, novel, predicted GTPase. *Cell* 90, 121–129.
- Hanson, G. T., Aggeler, R., Oglesbee, D., Cannon, M., Capaldi, R. A., Tsien, R. Y., and Remington, S. J. (2004). Investigating mitochondrial redox potential with redox-sensitive green fluorescent protein indicators. *J. Biol. Chem.* 279, 13044–13053.
- Hardie, D. G., Salt, I. P., Hawley, S. A., and Davies, S. P. (1999). AMP-activated protein kinase: an ultrasensitive system for monitoring cellular energy charge. *Biochem. J.* 338(Pt 3), 717–722.
- Hermann, G. J., Thatcher, J. W., Mills, J. P., Hales, K. G., Fuller, M. T., Nunnari, J., and Shaw, J. M. (1998). Mitochondrial fusion in yeast requires the transmembrane GTPase Fzo1p. *J. Cell Biol.* 143, 359–373.
- Hu, Q., Xia, Y., Corda, S., Zweier, J. L., and Ziegelstein, R. C. (1998). Hydrogen peroxide decreases pHi in human aortic endothelial cells by inhibiting Na<sup>+</sup>/H<sup>+</sup> exchange. *Circ. Res.* 83, 644–651.
- Ichishita, R., Tanaka, K., Sugiura, Y., Sayano, T., Mihara, K., and Oka, T. (2008). An RNAi screen for mitochondrial proteins required to maintain the morphology of the organelle in *Caenorhabditis elegans*. *J. Biochem.* 143, 449–454.
- Ihle, E. C., and Patneau, D. K. (2000). Modulation of alpha-amino-3-hydroxy-5-methyl-4-isoxazolepropionic acid receptor desensitization by extracellular protons. *Mol. Pharmacol.* 58, 1204–1212.
- James, D. I., Parone, P. A., Mattenberger, Y., and Martinou, J. C. (2003). hFis1, a novel component of the mammalian mitochondrial fission machinery. *J. Biol. Chem.* 278, 36373–36379.
- Kamath, R. S., Martinez-Campos, M., Zipperlen, P., Fraser, A. G., and Ahringer, J. (2001). Effectiveness of specific RNA-mediated interference through ingested double-stranded RNA in *Caenorhabditis elegans*. *Genome Biol.* 2, RESEARCH0002.
- Kanazawa, T., Zappaterra, M. D., Hasegawa, A., Wright, A. P., Newman-Smith, E. D., Buttle, K. F., McDonald, K., Mannella, C. A., and van der Bliek, A. M. (2008). The *C. elegans* Opa1 homologue EAT-3 is essential for resistance to free radicals. *PLoS Genet.* 4, e1000022.
- Kaufman, D. S., Goligorsky, M. S., Nord, E. P., and Graber, M. L. (1993). Perturbation of cell pH regulation by H<sub>2</sub>O<sub>2</sub> in renal epithelial cells. *Arch. Biochem. Biophys.* 302, 245–254.
- Kiss, L., and Korn, S. J. (1999). Modulation of N-type Ca<sup>2+</sup> channels by intracellular pH in chick sensory neurons. *J. Neurophysiol.* 81, 1839–1847.
- Kowald, A., Jendrach, M., Pohl, S., Bereiter-Hahn, J., and Hammerstein, P. (2005). On the relevance of mitochondrial fusions for the accumulation of mitochondrial deletion mutants: a modelling study. *Aging Cell* 4, 273–283.
- Lee, Y. J., Jeong, S. Y., Karbowski, M., Smith, C. L., and Youle, R. J. (2004). Roles of the mammalian mitochondrial fission and fusion mediators Fis1, Drp1, and Opa1 in apoptosis. *Mol. Biol. Cell* 15, 5001–5011.
- Li, J., and Eastman, A. (1995). Apoptosis in an interleukin-2-dependent cytotoxic T lymphocyte cell line is associated with intracellular acidification. Role of the Na(+)/H(+)-antiporter. *J. Biol. Chem.* 270, 3203–3211.

- Li, Z., Okamoto, K., Hayashi, Y., and Sheng, M. (2004). The importance of dendritic mitochondria in the morphogenesis and plasticity of spines and synapses. *Cell* 119, 873–887.
- Ludwig, M. G., Vanek, M., Guerini, D., Gasser, J. A., Jones, C. E., Junker, U., Hofstetter, H., Wolf, R. M., and Seuwen, K. (2003). Proton-sensing G-protein-coupled receptors. *Nature* 425, 93–98.
- Marsin, A. S., Bertrand, L., Rider, M. H., Deprez, J., Beauloye, C., Vincent, M. F., Van den Berghe, G., Carling, D., and Hue, L. (2000). Phosphorylation and activation of heart PFK-2 by AMPK has a role in the stimulation of glycolysis during ischaemia. *Curr. Biol.* 10, 1247–1255.
- Marsin, A. S., Bouzin, C., Bertrand, L., and Hue, L. (2002). The stimulation of glycolysis by hypoxia in activated monocytes is mediated by AMP-activated protein kinase and inducible 6-phosphofructo-2-kinase. *J. Biol. Chem.* 277, 30778–30783.
- Matsuyama, S., Llopis, J., Deveraux, Q. L., Tsien, R. Y., and Reed, J. C. (2000). Changes in intramitochondrial and cytosolic pH: early events that modulate caspase activation during apoptosis. *Nat. Cell Biol.* 2, 318–325.
- McDonald, J. W., Bhattacharyya, T., Sensi, S. L., Lobner, D., Ying, H. S., Canoniero, L. M., and Choi, D. W. (1998). Extracellular acidity potentiates AMPA receptor-mediated cortical neuronal death. *J. Neurosci.* 18, 6290–6299.
- Meeusen, S., DeVay, R., Block, J., Cassidy-Stone, A., Wayson, S., McCaffery, J. M., and Nunnari, J. (2006). Mitochondrial inner-membrane fusion and crista maintenance requires the dynamin-related GTPase Mgm1. *Cell* 127, 383–395.
- Misgeld, T., Kerschensteiner, M., Bareyre, F. M., Burgess, R. W., and Lichtman, J. W. (2007). Imaging axonal transport of mitochondria in vivo. *Nat. Methods* 4, 559–561.
- Mozdy, A. D., McCaffery, J. M., and Shaw, J. M. (2000). Dnm1p GTPase-mediated mitochondrial fission is a multi-step process requiring the novel integral membrane component Fis1p. *J. Cell Biol.* 151, 367–380.
- Nakamura, U., Iwase, M., Uchizono, Y., Sonoki, K., Sasaki, N., Imoto, H., Goto, D., and Iida, M. (2006). Rapid intracellular acidification and cell death by H<sub>2</sub>O<sub>2</sub> and alloxan in pancreatic beta cells. *Free Radic. Biol. Med.* 40, 2047–2055.
- Nehrke, K. (2003). A reduction in intestinal cell pH<sub>i</sub> due to loss of the *Caenorhabditis elegans* Na<sup>+</sup>/H<sup>+</sup> exchanger NHX-2 increases life span. *J. Biol. Chem.* 278, 44657–44666.
- Olichon, A., et al. (2002). The human dynamin-related protein OPA1 is anchored to the mitochondrial inner membrane facing the inter-membrane space. *FEBS Lett.* 523, 171–176.
- Otsuga, D., Keegan, B. R., Brisch, E., Thatcher, J. W., Hermann, G. J., Bleazard, W., and Shaw, J. M. (1998). The dynamin-related GTPase, Dnm1p, controls mitochondrial morphology in yeast. *J. Cell Biol.* 143, 333–349.
- Ou-Yang, Y., Kristian, T., Møllergaard, P., and Siesjö, B. K. (1994). The influence of pH on glutamate- and depolarization-induced increases of intracellular calcium concentration in cortical neurons in primary culture. *Brain Res.* 646, 65–72.
- Pfeiffer, J., Johnson, D., and Nehrke, K. (2008). Oscillatory transepithelial H<sup>(+)</sup> flux regulates a rhythmic behavior in *C. elegans*. *Curr. Biol.* 18, 297–302.
- Salt, I. P., Johnson, G., Ashcroft, S. J., and Hardie, D. G. (1998). AMP-activated protein kinase is activated by low glucose in cell lines derived from pancreatic beta cells, and may regulate insulin release. *Biochem. J.* 335, 533–539.
- Santel, A., and Fuller, M. T. (2001). Control of mitochondrial morphology by a human mitofusin. *J. Cell Sci.* 114, 867–874.
- Serasinghe, M. N., and Yoon, Y. (2008). The mitochondrial outer membrane protein hFis1 regulates mitochondrial morphology and fission through self-interaction. *Exp. Cell Res.* 314, 3494–3507.
- Shah, M. J., Meis, S., Munsch, T., and Pape, H. C. (2001). Modulation by extracellular pH of low- and high-voltage-activated calcium currents of rat thalamic relay neurons. *J. Neurophysiol.* 85, 1051–1058.
- Shepard, K. A., and Yaffe, M. P. (1999). The yeast dynamin-like protein, Mgm1p, functions on the mitochondrial outer membrane to mediate mitochondrial inheritance. *J. Cell Biol.* 144, 711–720.
- Smirnova, E., Shurland, D. L., Ryazantsev, S. N., and van der Bliek, A. M. (1998). A human dynamin-related protein controls the distribution of mitochondria. *J. Cell Biol.* 143, 351–358.
- Smith, D. M. (1931). The ontogenic history of the mitochondria of the hepatic cell of the white rat. *J. Morphol. Physiol.* 52, 485–512.
- Song, Z., Ghochani, M., McCaffery, J. M., Frey, T. G., and Chan, D. C. (2009). Mitofusins and OPA1 mediate sequential steps in mitochondrial membrane fusion. *Mol. Biol. Cell* 20, 3525–3532.
- Spinazzi, M., et al. (2008). A novel deletion in the GTPase domain of OPA1 causes defects in mitochondrial morphology and distribution, but not in function. *Hum. Mol. Genet.* 17, 3291–3302.
- Syntichaki, P., Samara, C., and Tavernarakis, N. (2005). The vacuolar H<sup>+</sup>-ATPase mediates intracellular acidification required for neurodegeneration in *C. elegans*. *Curr. Biol.* 15, 1249–1254.
- Tan, F. J., Husain, M., Manlandro, C. M., Koppenol, M., Fire, A. Z., and Hill, R. B. (2008). CED-9 and mitochondrial homeostasis in *C. elegans* muscle. *J. Cell Sci.* 121, 3373–3382.
- Thomas, J. A., Buchsbaum, R. N., Zimniak, A., and Racker, E. (1979). Intracellular pH measurements in Ehrlich ascites tumor cells utilizing spectroscopic probes generated in situ. *Biochemistry* 18, 2210–2218.
- Tsai, K. L., Wang, S. M., Chen, C. C., Fong, T. H., and Wu, M. L. (1997). Mechanism of oxidative stress-induced intracellular acidosis in rat cerebellar astrocytes and C6 glioma cells. *J. Physiol.* 502, 161–174.
- Twig, G., et al. (2008). Fission and selective fusion govern mitochondrial segregation and elimination by autophagy. *EMBO J.* 27, 433–446.
- Verstreken, P., Ly, C. V., Venken, K. J., Koh, T. W., Zhou, Y., and Bellen, H. J. (2005). Synaptic mitochondria are critical for mobilization of reserve pool vesicles at *Drosophila* neuromuscular junctions. *Neuron* 47, 365–378.
- Wu, M. L., Tsai, K. L., Wang, S. M., Wu, J. C., Wang, B. S., and Lee, Y. T. (1996). Mechanism of hydrogen peroxide and hydroxyl free radical-induced intracellular acidification in cultured rat cardiac myoblasts. *Circ. Res.* 78, 564–572.
- Xiong, Z. G., et al. (2004). Neuroprotection in ischemia: blocking calcium-permeable acid-sensing ion channels. *Cell* 118, 687–698.
- Ying, W., Han, S. K., Miller, J. W., and Swanson, R. A. (1999). Acidosis potentiates oxidative neuronal death by multiple mechanisms. *J. Neurochem.* 73, 1549–1556.
- Yoon, Y., Krueger, E. W., Oswald, B. J., and McNiven, M. A. (2003). The mitochondrial protein hFis1 regulates mitochondrial fission in mammalian cells through an interaction with the dynamin-like protein DLP1. *Mol. Cell Biol.* 23, 5409–5420.
- Zanna, C., et al. (2008). OPA1 mutations associated with dominant optic atrophy impair oxidative phosphorylation and mitochondrial fusion. *Brain* 131, 352–367.
- Zha, X. M., Wemmie, J. A., Green, S. H., and Welsh, M. J. (2006). Acid-sensing ion channel 1a is a postsynaptic proton receptor that affects the density of dendritic spines. *Proc Natl. Acad. Sci. USA* 103, 16556–16561.
- Zuchner, S., et al. (2004). Mutations in the mitochondrial GTPase mitofusin 2 cause Charcot-Marie-Tooth neuropathy type 2A. *Nat. Genet.* 36, 449–451.